

Toward Energy Efficient Wireless Sensor Networks Using Pilot Periods for Collision Detection

Fawaz Alassery and Walid K. M. Ahmed

Abstract— Power consumption represents one of the most constraints which affect the design of WSNs, leading to various protocols and algorithms aimed at minimizing the power consumption and extending batteries' lifetime. Sensor nodes in a WSN transmit their periodic packets continuously to cluster head nodes (receivers) which are responsible for processing and transferring packets to another parts of a network. In fact, cluster head nodes in WSNs most often consume a large amount of power due to the necessity to decode every received packet regardless of the fact that the transmission may suffer from packets collision which impede the network performance. Therefore, in the receiver side of WSNs current collision detection mechanisms have largely been revolving around direct demodulation and decoding of received packets and deciding on a collision based on some form of parity bits for error control. Full decoding of received packets with error control bits at cluster head nodes can achieve an efficient usage of network capacity, however, such an approach represents a major burden on power-constrained sensors. In this paper, we propose novel power efficient and low complexity techniques which achieve a significant power saving at the expense of low throughput losses. Based on studying the received packets, cluster head nodes can make a fast decision to detect a collision without the need for full-decoding of the whole received packets. Theoretical and simulation results show that our proposed Pilot Periods (PP) techniques can significantly reduce the computational complexity as well as the power consumption over existing Full-Decoding (FD) algorithms.

Index Terms— WSN Techniques, Power Consumption in WSNs, WSN Protocols, Solving Packets Collision.

I. INTRODUCTION

WIRELESS Sensor Networks (WSNs) have become increasingly popular due to their various applications. WSNs nodes are usually deployed in remote areas to perform their functions. They mainly use broadcast communication and the network topology can change due to the fact that some nodes may be prone to fail. One of the key challenges in wireless sensor design is power consumption, since the nodes have limited power resources as they typically operate off of batteries that are difficult to replace or recharge [1]. Therefore, a considerable amount of research in WSNs has focused on power saving techniques including the proposal of various power-efficient designs of electronic transceiver circuitry [2] and power-efficient Medium Access Control (MAC) protocols [5].

The need to extend the lifetime of sensors is a key challenge in designing current wireless sensor network (WSNs). In the literature, power conservation algorithms play very important role in order to extend the lifetime of WSN nodes, where typically such algorithms attempt at saving power by applying the power saving technique at either the transmitter or the receiver side. For example, using a strong error Correcting Code (ECC) at the transmitter results in a more reliable reception with a lower Signal-to-Interference-plus-Noise Ratio (SINR). However, this comes at the price of increasing the processing overhead (hence, also translating into increased power consumption) due to having to decode collision corrupted transmissions before knowing that such transmissions are corrupt, in addition to the high computational complexity that is required for using a strong ECC [12]. Consequently, in WSNs it is necessary to select appropriate channel coding schemes which simultaneously maintain low complexity and low power consumption for the sensor nodes. In [4], authors proposed a distributed algorithm for turbo coding/decoding in WSNs. The algorithm is based on using parallel concatenation convolutional codes over a noisy channel. In [6], the decoding computational complexity at the receiver in WSNs can be decreased via a proposed Viterbi Algorithm for Distributed Source Coding (VA-DSC). Authors in [8] proposed an energy-efficient Multiple Input Turbo (MIT) code for WSNs, the code can be used to reduce the amount of bit transmitted from sensor nodes, leading to power saving and better bandwidth utilization. In addition, in order to save power at the receiver, it is necessary to avoid decoding of packets which involve in collisions. However, with existing decoding algorithms in WSNs the total delay and power consumption to decode the received packets will be maximized due to the need to expend a significant amount of energy and processing complexity in order to fully-decode a packet, only to discover the packet is illegible due to a collision.

In wireless networks the most popular strategies to deal with packet collisions use the combination between carrier sensing and collision avoidance. In carrier sensing, all nodes in the network share the same transmission medium, a node starts with listening to the medium before transmitting its own packets in a pre-specified time period, which is determined by an access point (e.g. a central node in WSNs). If the state of the transmission medium is busy, a node takes a random backoff time and then continues transmitting its packets in order to avoid collisions with other nodes which are listening and contending for the medium as well. However, when the collision avoidance fails to detect corrupted packets, network resources such as the channel bandwidth and the system throughput will be wasted and decreased respectively due to the fact that some

Manuscript received December 8, 2015; revised December 30, 2015. This work has been sponsored by the Taif University of the Kingdom of Saudi Arabia.

Authors are with the Computer Engineering Department, Taif University, Saudi Arabia. (email: falassery@tu.edu.sa).

corrupted packets are still transmitted in their entirety. This situation may exacerbate since the rate of collision may increase with increasing the number of transmitters (e.g. sensors which have packets ready to transmit) [9].

Distributed MAC protocols such as the IEEE 802.11 Distributed Coordination Function (DCF) are widely used in wireless networks due to their simplicity of deployment. The protocols enable nodes to statistically share the wireless channel when transmitting their packets. However, the critical drawback of distributed MAC protocols is the inability to detect corrupted packets while nodes are transmitting. Therefore, IEEE 802.11 DCF employs a scheme called "virtual carrier sensing" which is based on in-bound control frames that are sent from a source (i.e. Request To Send (RTS) frame) to reserve the medium before sending the data frame [10]. When a receiver receives the RTS frame and declares the channel state as ready to receive packets, it responds with sending out another control frame (i.e. Clear To Send (CTS) frame) that reserves the channel for the sender. After that, the source will begin transmitting the data frames as long as the transmission medium is still reserved and the handshake mechanisms are processed successfully. In fact, several situations make the use for virtual carrier sensing difficult and inefficient for WSNs. One situation is the case which is called "chained" hidden nodes where the CTS frames may not be received by all hidden nodes (e.g. CTS frames are lost), which are not in the range of the initiating sender. So, some hidden nodes may not be suppressed. Another phenomenon that may impact the effectiveness of virtual carrier sensing is the node mobility. When a node moves into a neighborhood and misses the reservation information, it may become un-suppressed hidden node to the on-going handshake communication [10]. Hence, solving hidden nodes to prevent collision in WSNs has been researched extensively in literatures, some proposed MAC protocols used an out-of-band control channel to suppressed hidden nodes through sending control signals only when necessary [11]. These protocols rely on a single data channel where control frames are prevented from the transmission when the data frames are in a delivering state.

The MAC layer in WSNs needs to be a well-defined due to the fact that sensors are more energy consuming as they must be remain active all time to perform their functions such as sensing and processing the periodic tasks. Therefore, some proposed MAC algorithms consider the power consumption strategies to extend the lifetime of sensors as the main constraint in designing WSNs. Hence, WSNs designers need to keep in mind the energy efficiency in order to extend the duration of the network and enhance the overall system throughput. In addition, energy efficient MAC protocols in WSNs need to be finely accommodative to any change may occur in the network such as increasing or decreasing the number of nodes, changing the network topology and the bandwidth utilization [12].

The most popular MAC protocols in WSNs are investigated in the literature and categorized into S-MAC, SIFT, DMAC, T-MAC and DS-MAC protocols. First, the basic concept of Sensor-MAC (S-MAC) protocol is the synchronization and the scheduling of sleep and listen states among all nodes in the networks. S-MAC protocol relays on dividing the network into clusters where there is one cluster head that manages scheduling between sensor nodes which

are close to each other. The main disadvantage of this protocol is the large amount of energy consumed due to the fact that if there is two neighboring nodes reside in two different clusters, they need to follow two different scheduling mechanisms (i.e. one scheduling mechanism for each cluster). This results in extra listening and overhearing which may increase the number of scheduling packets in the network and hence cause a collision. Another disadvantage of S-MAC protocol is increasing the network latency. That is when two nodes are located in clusters which are not close to each other. In addition, decreasing the algorithm efficiency is expected in S-MAC protocol since each node has its own pre-defined sleep and listen schedules that are not accommodative to the variable traffic load. Moreover, the probability of collision increases due to the use of the simple collision avoidance strategy, i.e., the RTS/CTS control signals didn't used when broadcasting data packets [13].

Second, for event-driven WSNs, SIFT protocol is proposed based on the idea that when an event is sensed in a specific area covered by M sensors, the first group of M packets is considered as the highest priority packets and needed to be delivered as fast as possible with low latency. The major disadvantage of SIFT protocol that contradicts with main challenge in designing WSNs is remaining all nodes in busy states since the necessity for sensing all events occur in the network where there are no sleeping states. Hence, a large amount of energy is consumed when using such a MAC protocol [14].

Third, the proposal MAC protocol for data-gathering from sensors to an ultimate sink node is D-MAC protocol. It relies on a data-gathering tree which has unknown paths from a sensor transmitting its own packet to a sink node. The obvious drawback of this protocol is, the difficulty to detect a collision since neither collision avoidance strategy nor RTS/CTS control signals have been used [15].

Fourth, the Time-Out MAC protocol (T-MAC) is proposed to enhance the performance of the well-known S-MAC protocol through supporting heavy traffic load. A node may move to the sleeping state after a pre-defined time period if the medium is ideal and there is no event is occurred in the network (i.e. it relays on listening time threshold). The major disadvantage of such protocol is increasing the computational complexity and analysis which contradicts with the simplicity of WSNs. Also, carrier sensing with collision avoidance is the strategy used to detect a collision which is ineffective for WSNs [9].

Fifth, the dynamic duty cycle idea is added to S-MAC protocol to enable all nodes to start their transmission at the same duty cycle. This enhancement of S-MAC protocol is called Dynamic Sensor MAC protocol (DS-MAC). All nodes share their own one-hop latency values. If a sink node notices that the one hop latency value exceeds a specified threshold level, it sends messages to all sensors and requests decreasing of all sleeping periods. The high implementation complexity of DS-MAC is considered as the main disadvantage. In addition, the probability of collision increases due to the use of a simple carrier sense with collision avoidance strategy [16].

Thus, most of MAC protocols have been discussed above may suffer from some drawbacks that affect the performance of a limited energy resource network such as a

WSN. In addition, for all of these protocols and due to the need for fast transmission of packets, a simple carrier sensing with collision avoidance is used. However, carrier sensing with collision avoidance may increase the probability of collision that may occur because of some reasons such as the case when two sensors wake up simultaneously and choose the same back-off time, or the case when the nodes are hidden to each other.

In the light of above discussion, the study presented in this paper has been motivated. Current decoding algorithms used in WSNs may suffer from high computational complexities and power consumptions which affect the network performance. In addition, collision detection is one of the main sources of overhead power consumption in wireless sensors, since until the access node has expended the required power and processing-time to detect/decode the received packet, it wouldn't know that the packet has suffered a collision. In this paper, we propose a suite of novel, yet simple and power-efficient techniques to detect a collision without the need for full-decoding of the received packet. Our novel approaches aim at detecting collision through fast examination of a short snippet of the received packet via a relatively small number of computations over a small number of received IQ samples. Hence, operating directly at the output of the receiver's analog-to-digital-converter (ADC) and eliminating the need to pass the signal through the entire demodulator/decoder line-up. Accordingly, our novel approach not only reduce processing complexity and hence power consumption, but they also reduce the latency incurred to detect a collision since they operate on only a small number of samples that may be chosen to be in the beginning of a received packet - instead of having to buffer and process the entire packet as is the case with a full-decoding approach. Furthermore, our approaches operate directly on the (random) data, i.e., the received packet as is. We also present a complexity and power-saving comparison between our novel approaches and conventional full-decoding (for select coding schemes) to demonstrate the significant power and complexity saving advantage of our approaches. In addition, we show that with a relatively short measurement period, our schemes can achieve low Miss and False-Alarm probabilities. Hence, achieving a reliable collision-detection mechanism for WSNs. We also show how to tune various design parameters in order to allow a system designer multiple degrees of freedom for design trade-offs and optimization.

The remainder of this paper is organized as follows. In Section II we reviews some related works that focus on existing power efficient techniques in WSN's. Section III describes our system. In section IV, we explain our proposed PP techniques. In section V, we evaluate the power saving and system throughput based on our PP proposed approach. In addition, we compare the computational complexity of our PP approach against commonly used FD algorithms. In section VI, we present performance results, and finally in section VII we provide the conclusion for this paper.

II. RELATED WORKS

There are various sources of overhead power consumption in WSNs. For example, sensor nodes consume power when in idle mode, i.e., waiting and listening for packets to be

received, but not transmitting. Another cause for overhead energy loss in WSNs is the reception of packets which are not addressed to a node, and re-transmission of control packets, which is considered as protocol overhead [17]. One of the main sources of overhead power consumption in wireless sensors, which is the focus of this paper, is collision detection. When multiple sensors transmit at the same time, their transmitted packets collide at the central (e.g., access) node. However, until the access node has expended the required power and processing-time to detect the received packet, it wouldn't know that the packet is invalid and corrupted due to collision.

Various studies in the literature are aimed at maximizing the lifetime of WSNs nodes and reducing their power consumption. Generally, such techniques can be classified into four main categories. The first focuses on efficient routing protocols, such as the algorithm proposed in [18] which evaluates the interference from neighboring nodes and routes the packets through the least interference-prone path. In [19] a direct diffusion routing protocol is proposed, which constructs a routing tree via a Geo-cast approach when a failure occurs in the routing path. A comprehensive survey of energy-saving routing protocols for WSNs can be found in [20].

The second category of energy saving techniques focuses on efficient scheduling. For example, a sensor can switch from a "sleep" state to an "active" state when a packet is expected to be received. In [21], the authors divide a WSN into sets; the sensors monitor a target at specific time slots while other sets contain sensors which are scheduled to be in a sleeping mode. Authors in [22] proposed a contiguous link scheduling approach which uses TDMA where a time slot is allocated to each sensor when transmitting its packets.

The third category of energy saving techniques focuses on reducing power consumption in WSNs via efficient compression of transmitted packets to reduce the required bit-rate. For example, the authors in [23] propose a technique in which packets can be compressed and routed to a reduced list of dominant sensor receivers. Hence, packets do not need to be processed by unnecessary sensors. In [24], the authors propose low-energy adaptive clustering hierarchy (LEACH) approach, which is a protocol that aims at aggregating the information being transported, and dividing the sensor network into clusters where the energy load can be distributed amongst the nodes in each cluster.

The last category of power saving techniques in WSNs attempts at controlling the network topology via tuning the transmission power while maintaining the connectivity among nodes. For example, in [25], the authors propose a local minimum spanning tree (LMST) protocol to control wireless multi-hop topology. Basically, each node builds its own tree independently using locally collected data, their simulation results show that the LMST protocol can increase the network capacity as well as reduce the energy consumption.

III. SYSTEM DESCRIPTION

Figure 1 depicts an example of a WSN where a number of intermediate sensors are deployed arbitrarily to perform certain functionalities including sensing and/or collecting data and then communicating such information to a central sensor node (e.g. cluster head node) [30]. The central node

may process and relay the aggregate information to a backbone network.

As seen in Figure 1, there are N wireless sensors that communicate to the central sensor node, where at any point in time, multiple sensors may accidentally transmit simultaneously and cause a collision¹. Without loss of generality, we shall assume for the sake of argument that one sensor is denoted a “desirable” sensor, while the rest of the colliding sensors become “interferers”.

A commonly accepted model for packet arrivals, i.e., a packet is available at a sensor and ready to be transmitted, is the well-known Bernoulli-trial-based arrival model, where at any point in time, the probability that a sensor has a packet ready to transmit is P_{Tr} ².

Upon the receipt of a packet, the central node processes and evaluates the received packet and makes a decision on whether the packet is a collision-free (good) or has suffered a collision (bad). In this paper, we propose a suite of fast collision detection techniques where the central node evaluates the statistics of the received signal’s IQ samples at the output of the receiver’s analog-to-digital converter (ADC) directly using simple discrimination metrics, as will be explained in more detail in the following sections, saving the need to expend power and time on the complex modem line-up processing (e.g., demodulation and decoding). If the packet passes the PP approach test, it is deemed collision-free and undergoes all the necessary modem processing to demodulate and decode the data. Otherwise, the packet is deemed to have suffered a collision, which in turn triggers the central node to issue a NACK message per the mechanism and rules mandated by the specific multiple-access scheme employed in the network.

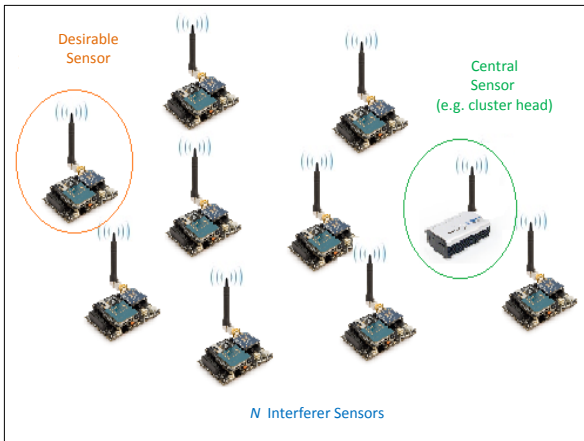


Fig.1. Wireless Sensor Network (WSN) with one desirable sensor, N interferer sensors and a central sensor.

IV. TECHNIQUES DESCRIPTION

As mentioned earlier, our proposed algorithm is based upon evaluating the statistics of the received signal at the receiver ADC output via the use of a simple statistical discrimination approach calculation that is performed on a relatively small portion of the received IQ packet samples. The resulting

¹ We assume the maximum number of sensors i.e. $N=30$. This number can be tuned as required in order to meet designers’ requirements.

² The actual design details and choice of the multiple access mechanism, e.g., slotted or un-slotted Aloha, are beyond the scope of this paper and irrelevant to the specifics of the techniques proposed herein.

approach value is then compared with a pre-specified threshold to determine if the statistics of the received samples reflect an acceptable Signal-to-Interference-plus-Noise Ratio (SINR) from the decoding mechanism perspective. If so, the packet is deemed collision-free and qualifies for further decoding. Otherwise, the packet is deemed to have suffered a collision with other interferer(s) and is rejected without expending any further processing/decoding energy. A repeat request may then be issued so the transmitting sensors to re-try depending on the MAC scheme. In other words, the idea is to use a fast and simple calculation to determine if the received signal strength (RSS) is indeed due to a single transmitting sensor that is strong enough to achieve an acceptable SINR at the central node’s receiver, or the RSS is rather due to the superposition of the powers of multiple colliding packets, hence the associated SINR is less than acceptable to the decoding mechanism.

Let’s define the k^{th} received signal (complex-valued) IQ sample at the access node as:

$$y_k = x_{0,k} + \sum_{m=1}^{N-1} x_{m,k} + n_k$$

where

$$y_k = y_{k,I} + j y_{k,Q}, j = \sqrt{-1},$$

$$x_{0,k} = x_{0,k,I} + j x_{0,k,Q}$$

is a complex-valued quantity that represents the k^{th} IQ sample component contributed by the desired sensor, while

$$x_{m,k} = x_{m,k,I} + j x_{m,k,Q}; m = 1, \dots, N-1$$

is the k^{th} IQ sample component contributed by the m^{th} interfering (colliding) sensor. Finally, $n_k = n_{k,I} + j n_{k,Q}$ is a complex-valued Additive-White-Gaussian Noise (AWGN) quantity (e.g., thermal noise).

We propose two Pilot Periods (PP) schemes that are applied to the envelope value, $|y_k| = \sqrt{y_{k,I}^2 + y_{k,Q}^2}$, of the received IQ samples at the central node as detailed in the following subsections.

A. Zero-Power Periods Transmission

The scheme is based on zero-power periods transmission as it will be explained further below. For the sake of case study we assume the following:

- Let the transmitted packet be divided into U periods (i.e. slots) where each packet has Z zero-power periods (i.e. power-off slots which carry neither information nor power) and D actual data periods (i.e. power-on slots).
- We form $C(U,Z) \geq N$ possible (distinct) zero-power periods combination (i.e. each sensor transmitted packet has its own zero-power periods in locations that can be overlapped with some zero-power periods for packets transmitted from other sensors).
- let L_k is the maximum possible size (or length) of the transmitted packet; $L_k = 1, 2, \dots, K$. Also, let L_g is the length of the zero power period³; $L_g = 1, 2, \dots, G$, and L_S is the length of the actual data period; $L_S = 1, 2, \dots, S$.

³ We assume the length of the zero-power period (L_g) is 5% of the total number of samples. In our design we try to minimize L_g as much as possible without degradation in the system performance.

- We assume T_l and H_h represent the l^{th} and h^{th} zero power period and actual data period respectively; $l=1,2,\dots,Z$ and $h=1,2,\dots,D$.
- The absolute power is assumed to be the minimum average power over all packet's slots which have been checked by the central node. It can be defined as:

$$\eta_{\text{Pilot}} = \min \left(\sum_{l=1}^Z \left(\frac{1}{G} \sum_{g=1}^G |P_g| \right), \sum_{h=1}^D \left(\frac{1}{S} \sum_{s=1}^S |P_s| \right) \right) \quad (1)$$

where

$$P_g = |y_{k,i}|^2; \quad i=1,2,\dots,G$$

$$P_s = |y_{k,j}|^2; \quad j=1,2,\dots,S$$

Figure 2 shows an example for packets which are transmitted from different sensors where zero-power periods may overlap in their locations.

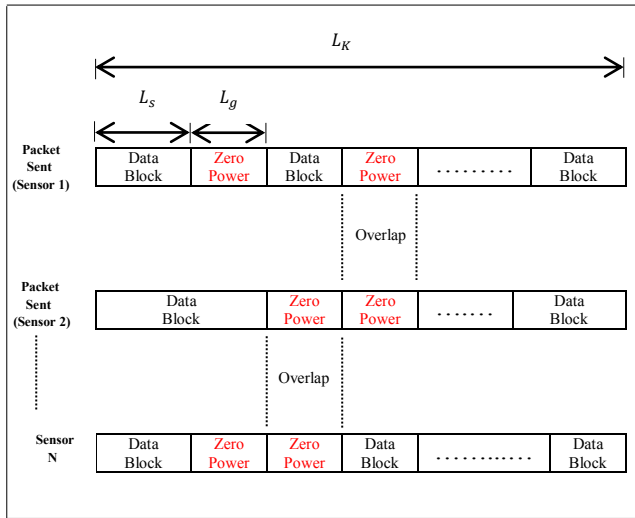


Fig.2. Example of a packet structure for the zero-power periods scheme.

Upon the receipt of a packet, the sink node sweeps all possible zero-power and actual data periods for a packet in order to find the absolute power (η_{Pilot}) and hence compares it with a pre-specified threshold level (γ) that is set based on a desired Signal to Interference plus Noise Ratio (SINR) cut-off assumption ($SINR_{\text{cut_off}}$)⁴ as will be described in more detail later in this paper. That is a system designer pre-evaluates the appropriate threshold value that corresponds to the desired $SINR_{\text{cut_off}}$. If η_{Pilot} is higher than the threshold value, then the PP approach value reflects a SINR that is less than $SINR_{\text{cut_off}}$ and the packet is deemed not usable, and vice-versa. Accordingly, a “False-Alarm” event occurs if the received SINR is higher than $SINR_{\text{cut_off}}$ but the PP approach erroneously deems the received SINR to be less than $SINR_{\text{cut_off}}$. On the other hand, if the PP approach deems the SINR to be higher than $SINR_{\text{cut_off}}$ while it is actually less than $SINR_{\text{cut_off}}$, a “Miss” event is encountered. Miss and False-Alarm probabilities directly impact the overall system performance as will be discussed in the following sections. Therefore, it is desired to minimize such probabilities as much as possible.

⁴ In order to have a threshold setting that is independent of the absolute level of the received signal power (hence independent of path loss, receiver gain ...etc.) the collected IQ samples of the measurement period may first be normalized to unity power.

B. Single Pseudo-Coded On-OFF Pilot Period Transmission

This scheme is based on a single pseudo-coded ON-OFF pilot period per packet. Figure 3 depicts a pictorial illustration of the packet structure for the single pilot period scheme. In the single pilot scheme we assume the following:

- A distinct sequence per sensor. That is, $PNP_i \neq PNP_j; i \neq j$.
- PNP_j must have the same duty-cycle (D) for all $1 \leq j \leq N$.
- The length of the actual data block is L_{max} , and the length of the pilot period (PNP_j) is L .
- L is divided into ν slots which include ν_z all zeros slots and ν_o all ones slots, i.e., we assume the same ratio of ν_z to ν_o as well as different ratio (e.g. 40%,50%, etc.). Accordingly, we evaluate different length of L based how many ν and ω (i.e. $L = \nu \times \omega$). In our design we try to minimize L as much as possible and ensure the PP approach would still work reliably. For example, we assume $\nu=8$ slots and $\omega=2$ samples, so $L=16$ samples (It can be tuned as required by a designer).
- The central node is aware of what transmitted PNP_j period to expect for each sensor.
- We evaluate various “soft” decision percentages (i.e. \aleph) when decoding the pilot period at the central node. We quantify the effect and performance versus different \aleph such as 60%,70% and 90% (It can be tuned as required by a designer).
- The relative power is assumed to be the average power for the actual data block to the average power for the pseudo-coded ON-OFF pilot period. It can be defined as:

$$\eta_{\text{Pilot}} = \frac{\left(\frac{1}{L_{\text{max}}} \sum_{i=L+1}^{L_{\text{max}}} P_i \right)}{\left(\frac{1}{L} \sum_{j=1}^L P_j \right)} \quad (2)$$

where

$$P_i = |y_{k,i}|^2; \quad i=L+1, L+2, \dots, L_{\text{max}}$$

$$P_j = |y_{k,j}|^2; \quad j=1, 2, \dots, L$$

In the single pilot period approach, the central node needs to decode (i.e. through ML detection) the pilot sequence for each received packet and compare it with the pre-stored look-up table (code-book) of all the valid sequences. If the sequence of the decoded pseudo-coded ON-OFF pilot period match \aleph (or more) of any pre-stored sequence, then the received packet is a collision-free packet, and vice versa.

For a collision-free packet and as we explained in previous technique, the relative power (η_{Pilot}) is compared with a pre-specified threshold value that is set based on $SINR_{\text{cut_off}}$. If η_{Pilot} is higher than the threshold value, then the PP approach value reflects a SINR that is less than $SINR_{\text{cut_off}}$ and the packet is deemed not usable, and vice-versa. Accordingly, a “False-Alarm” event occurs if the received SINR is higher than $SINR_{\text{cut_off}}$ but the PP approach erroneously deems the received SINR to be less than $SINR_{\text{cut_off}}$. On the other hand, if the PP approach deems the SINR to be higher than $SINR_{\text{cut_off}}$ while it is actually less than $SINR_{\text{cut_off}}$, a “Miss” event is encountered.

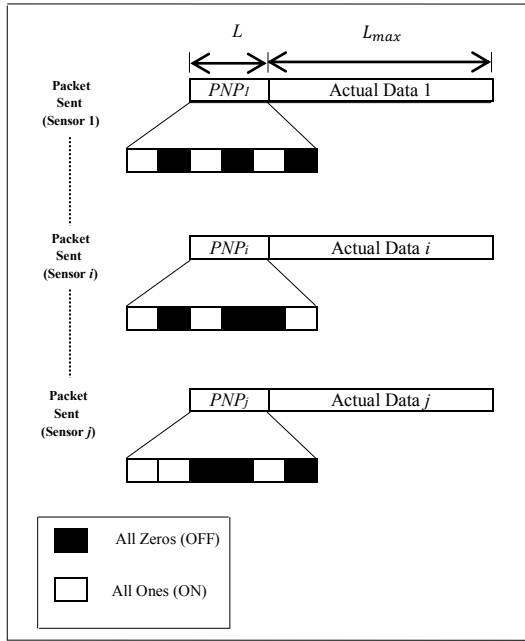


Fig.3. Example of a packet structure for the single pseudo-coded ON-OFF pilot period.

In the following we show how to decode the single pseudo-coded ON-OFF pilot period through the Maximum Likelihood (ML) detection [3]. Let the transmitted block be x_k ; $k=1,2,\dots,L_{max}$, and the received block be y_k ; $k=1,2,\dots,L_{max}$. As mentioned earlier, the k^{th} received signal (complex-valued) IQ sample at the central node is:

$$y_k = x_{0,k} + \sum_{m=1}^{N-1} x_{m,k} + n_k$$

where $x_{0,k}$ is a complex-valued quantity that represents the k^{th} IQ sample component contributed by the desired sensor, while $x_{m,i}$ is the k^{th} IQ sample component contributed by the m^{th} interfering (colliding) sensor. Finally, n_k is a complex-valued Additive White Gaussian Noise (AWGN) quantity. Accordingly, the channel transition probability density function (pdf) $P(y_k|x_k)$ is:

$$P(y_k|x_k) = \frac{1}{(2\pi\sigma^2)^{L_{max}}} \exp\left(-\frac{1}{2\sigma^2} \sum_{k=1}^{L_{max}} |y_k - x_k|^2\right) \quad (3)$$

Hence, ML detection algorithm needs to maximize $P(\bar{y}_k|\bar{x}_k)$, i.e., similar to (3) for all received packets, where in this case \bar{y}_k is the vector for the received pilot period, and \bar{x}_k is the vector for the transmitted pilot period. Equivalently, ML detector can maximize the log-likelihood function for the pilot period as follows:

$$\begin{aligned} \mathcal{F}_r &\propto \left(P(\bar{y}_k|\bar{x}_k)\right) \\ &= -\sum_{k=1}^L |\bar{y}_k - \bar{x}_k|^2 \end{aligned}$$

The following procedures implement the ML detection for our proposed single pseudo-coded ON-OFF pilot period approach:

1. Start with $k=1$.
2. Calculate: $\mathcal{F}_r = -\sum_{k=1}^L |\bar{y}_k - \bar{x}_k|^2$
3. Store \mathcal{F}_r .
4. Increment k by one.
5. If $k=L+1$ go to step 7.
6. Go to step 2.
7. Find the sequence that correspond to the largest \mathcal{F}_r and declare it as the detected sequence (PNP_j).

As mentioned earlier, if the sequence PNP_j match \aleph (or

more) of any pre-stored sequence, then the corresponding received packet is declared as a collision free packet. For the collision free packet, η_{pilot} is compared with a pre-specified threshold level (i.e. set based on $SINR_{cut,off}$) in order to analyze packets' statistics (i.e. False-Alarm and Miss probabilities).

C. Threshold Selection

The decision threshold is chosen based on evaluating the False-Alarm and Miss probabilities and choosing the threshold values that satisfy the designer's requirements of such quantities. For example, we generate, say, a 100,000 Monte-Carlo simulated snapshots of interfering sensors (e.g., 1~30 sensors with random received powers to simulate various path loss amounts) where for each snapshot we compute the discrimination (PP) approach value (i.e. η_{pilot}) for the received $SINR$ and compare it with various threshold levels, determine if there is a corresponding False-Alarm or Miss event and record the counts of such events. At the end of the simulations the False-Alarm and Miss probabilities are computed and plotted versus the range of evaluated threshold values, which in-turn, enables the designer to determine a satisfactory set point for the threshold.

V. COMPUTATIONAL COMPLEXITY, POWER SAVING AND SYSTEM THROUGHPUT ANALYSIS

To analyze the power saving of our proposed PP system we introduce the following computational complexity metrics:

$$F_B = S + P_{miss} F \quad (4)$$

$$F_G = S + (1 - P_{FA}) F \quad (5)$$

In above formulas, S is the number of computational operations incurred in our proposed techniques, while F is the number of computational operations incurred in a Full-Decoding techniques (FD), P_{miss} and P_{FA} are the probabilities of Miss and False-Alarm events respectively. Hence, F_B represents the computational complexity for the case where the cluster head node makes a wrong decision to fully-decode the received packet (i.e., declared as a collision-free packets) while the packet should has been rejected (i.e., due to collision). On the other hand, F_G is the computational complexity for the case where the cluster head node makes a correct decision to fully decode received packet.

For the comparison purposes, we introduce the following formulae in order to compare the computational complexity saving achieved by the proposed PP approach (i.e. T_{PP}) over the FD approach (i.e. T_{FD}):

$$T_{PP} = F_B P_{collision} + F_G P_{no_collision} \quad (6)$$

$$T_{FD} = F \quad (7)$$

In above formulae, $P_{collision}$ and $P_{no_collision}$ are the probabilities of collision and no-collision events respectively. $P_{collision}$ and $P_{no_collision}$ have been obtained via Monte-Carlo simulation as follows: A random number of interfering sensors (maximum of 30 sensors) is generated per a simulation snapshot, where each sensor is assumed to have a randomly received power level at the cluster head node (to reflect a random path loss/location effect). The generation of the interfering sensors is based on a Bernoulli trial model where it is assume that the probability of a

packet available for transmission at a sensor (hence the existence/generation of the sensor for the snapshot at hand) is equal to α . If the total SINR is found to be worse than the cut-off limit, a collision is assumed and vice-versa. For our numerical example in this section we used $\alpha = 0.3$ and $SINR_{cut_off} = 5\text{dB}$. Also, we typically generate more than 100,000 snapshots in order to achieve a reliable estimate of the collision probabilities. For the aforementioned choices of α and $SINR_{cut_off}$, we found the collision probabilities to be $P_{collision} = 0.3649$ and $P_{no_collision} = 0.6351$.

A. Comparing with Full-Decoding

In order to assess the computational complexity of our PP techniques, we first quantize the PP calculations in order to define fixed-point and bit-manipulation requirements of such calculations. We also assume a look-up table (LUT) approach for the complexity analysis calculation. Note that the number of times the PP techniques need to access the LUT equals the number of IQ samples involved in the complexity calculation. Thus, our PP techniques only need to perform addition operations as many times as the number of samples. Hence, if the number of bits per LUT word/entry is equal to M at the output of the LUT, our PP techniques need as many M -bit addition operations as the number of IQ samples.

As a case-study, we compare the complexity of the proposed PP techniques with the complexity of FD algorithms assuming a log-MAP algorithm and a Max-log-MAP algorithm, respectively. These algorithms have been attractive choices for WSNs [26],[27]. Note that in the following analysis we will compare the zero power period technique against the log-MAP algorithm, also we will compare the single pilot period technique against the Max-log-MAP algorithm. Authors in [28] measure the computational complexity of log-MAP and Max-log-MAP (per information bit of the decoded codeword) based on the size of the encoder memory. It has been shown that for a memory length of λ , the total computational complexity per information bit for log-MAP and Max-log-MAP algorithms can be estimated respectively as:

$$F_{\text{Log-MAP}} = 25 \times 2^\lambda + 13 \quad (8)$$

$$F_{\text{Max-Log-MAP}} = 15 \times 2^\lambda + 17 \quad (9)$$

In contrast, our PP system does not incur such complexity related to the size of the encoder memory. In addition, our PP system avoids other complexities required by a full decoding such as time and frequency synchronization, Doppler shift correction, fading and channel estimation, etc., since our PP approaches operate directly at the IQ samples at the output of the ADC "as is". Finally, the FD approaches require buffering and processing of the entire packet/codeword while our PP approaches need only to operate on a short portion of the received packet.

Now let's compute the computational complexity for our PP techniques. Let's assume that the IQ ADCs each is D bits. Also, let's assume a $(\cdot)^2$ operation is done through a LUT approach to save multiplication operations. In addition, let's also assume that the square-root, $\sqrt{\cdot}$, is also done through a LUT approach. Hence, each of the I^2 and Q^2

operations consume of the order of D bit-comparison operations to address the $(\cdot)^2$ LUT. Then, if the output of the LUT is G bits, it follows that we need about G bit additions for an $I^2 + Q^2$ operation. Let's assume that the $\sqrt{\cdot}$ LUT has G bits for input addressing and K output bits. Then, we need about $G+1$ bit-comparison operations to address the $\sqrt{\cdot}$ LUT. Finally, for simplicity, let's assume that a bit comparison operation costs as much as a bit addition operation⁵. Accordingly, the total number of operations needed to compute the $(\sqrt{I^2 + Q^2})$ for one IQ sample is:

$$2D + G + (G + 1) = 2D + 2G + 1 \quad (10)$$

However, our approaches are based on calculating the power for the pilot period(s) and the actual data period(s). So, the total number of operations needed to compute the $(I^2 + Q^2)$ for one IQ sample (E) is:

$$E = 2D + G \quad (11)$$

If we assume the IQ over-sampling rate (OSR) to be Z (i.e., we have Z samples per information symbol), then we need about $Z \times G$ bit additions to add the $Z(I^2 + Q^2)$ values for every information symbol. Hence, for one information symbol, we need a total of:

$$(2D + G) \times Z + Z \times G = (2D + 2G)Z \quad (12)$$

Now if we assume an M -ary modulation (i.e., $\log_2 M$ information bits are mapped to one symbol), then the computational complexity per information bit can be computed as:

$$S / \text{InfoBit} = \frac{(2D + 2G)Z}{\log_2(M)} \quad (13)$$

For example, in order to show the complexity saving of our PP techniques, let's assume a QPSK modulation scheme ($M=4$). Also, let's assume $Z=2$ (2 samples per symbol), and $D = G = 10$ bits, which represents a good bit resolution. Also, let's assume a memory size of $\lambda = 5$ for the Log-MAP and Max-Log-MAP decoders. Using the formulae (8) and (9), it follows the Log-MAP FD algorithm costs 813 operations per an information bit, and the MAX-Log-MAP FD algorithm costs 497 operations per an information bit, while our PP techniques based on formula (13) costs only 40 operations per an information bit, which represents a 95% and a 91% saving on the computational complexity over log-MAP and Max-log-MAP algorithms, respectively.

In addition, in a no-collision event, the PP techniques check would represent a processing overhead. Nonetheless, our PP techniques still provide a significant complexity saving over the FD techniques as demonstrated by the following example. Table II in Appendix A shows the probability of Miss and False-Alarm to be 0.0926 and 0.0921, respectively, for the zero-power periods technique, QPSK and 1000 bits measurement period. In addition, table V in the in Appendix A shows the probability of Miss and False-Alarm to be 0.0712 and 0.0718, respectively, for the single pilot period technique, QPSK, $\kappa=70\%$, and 50 bits measurement period. Now, based on formulae (4) and (5), F_B and F_G (per information bit) for our PP techniques

⁵ Similar assumptions were made in [28].

against log-MAP and Max-log-MAP algorithms respectively are equal:

$$\begin{aligned} F_{B,Zero_Power} &= S + P_{miss} F_{Log-MAP} \\ &= 40 + 0.0926 \times 813 \\ &= 115 \text{ Operations per Info Bit} \end{aligned}$$

$$\begin{aligned} F_{G,Zero_Power} &= S + (1 - P_{FA}) F_{Log-MAP} \\ &= 40 + (1 - 0.0921) \times 813 \\ &= 778 \text{ Operations per Info Bit} \end{aligned}$$

$$\begin{aligned} F_{B,Single_Pilot} &= S + P_{miss} F_{Max-Log-MAP} \\ &= 40 + 0.0712 \times 497 \\ &= 75 \text{ Operations per Info Bit} \end{aligned}$$

$$\begin{aligned} F_{G,Single_Pilot} &= S + (1 - P_{FA}) F_{Max-Log-MAP} \\ &= 40 + (1 - 0.0718) \times 497 \\ &= 501 \text{ Operations per Info Bit} \end{aligned}$$

For the comparison purposes between our PP techniques and FD algorithms (i.e. the Log-MAP and the Max-Log-MAP, respectively), formulae (6) and (7) are used to find the computational complexity when no-collision is detected:

$$\begin{aligned} T_{PP,Zero_Power} &= F_{B,1} P_{collision} + F_{G,1} P_{no_collision} \\ &= 115 \times 36.49\% + 778 \times 63.51\% \\ &= 536 \text{ Operations per Info Bit} \end{aligned}$$

$$\begin{aligned} T_{FD,Zero_Power} &= F_{Log-MAP} \\ &= 813 \text{ Operations per Info Bit} \end{aligned}$$

$$\begin{aligned} T_{PP,Single_Pilot} &= F_{B,2} P_{collision} + F_{G,2} P_{no_collision} \\ &= 75 \times 36.49\% + 501 \times 63.51\% \\ &= 345 \text{ Operations per Info Bit} \end{aligned}$$

$$\begin{aligned} T_{FD,Single_Pilot} &= F_{Max-Log-MAP} \\ &= 497 \text{ Operations per Info Bit} \end{aligned}$$

Hence, the complexity savings (in number of operations per information bit) against the Log-MAP and Max-Log-MAP algorithms becomes respectively as:

$$\begin{aligned} \Delta_{PP,Zero_Power} \% &= (T_{FD,1} - T_{PP,1}) / T_{FD,1} \\ &= (813 - 536) / 813 = 34.07 \% \end{aligned}$$

$$\begin{aligned} \Delta_{PP,Single_Pilot} \% &= (T_{FD,2} - T_{PP,2}) / T_{FD,2} \\ &= (497 - 345) / 497 = 30.58 \% \end{aligned}$$

Figures 4 and 5 show the corresponding power saving percentage per information bit for various bit resolutions (e.g. 8,9,10,11 and 12 bits) of our PP techniques over the FD algorithms (i.e. the Log-MAP and the Max-Log-MAP) when the encoder memory size (λ) = 4 and 5, respectively.

Note that the above complexity saving calculations, in fact, represent a lower bound on the saving since the above calculations did not take into account the modem line-up operational complexity in order to demodulate and receive the bits in their final binary format properly (i.e., synchronization, channels estimation, etc.).

The performance of our techniques can be tuned as desired by a system designer. Appendix A provides performance comparisons for various examples where the system designer may have multiple degrees of freedom for design trade-offs and optimization.

Percentage for Power Saving per Information bit PP over FD, Memory size= 4

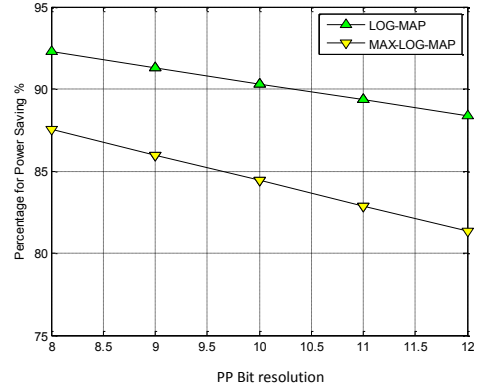


Fig. 4. Power saving percentage per information bit for PP techniques over FD techniques when the encoder memory size (λ)=4.

Percentage for Power Saving per Information bit PP over FD, Memory size= 5

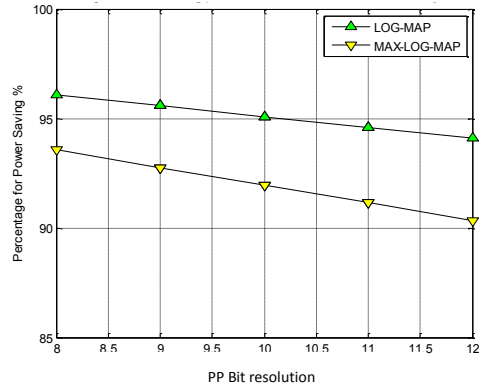


Fig. 5. Power saving percentage per information bit for PP techniques over FD techniques when the encoder memory size (λ)=5.

VI. RESULTS AND DISCUSSION

In this section we provide numerical performance evaluation of our proposed statistical discrimination techniques for various system design scenarios and parameter choices. We also consider three modulation techniques, namely, QPSK, 8PSK and 16PSK.

As pointed out in previous sections, without loss of generality and for the sake of a case study, we assume that a typical error correcting decoding scheme can successfully decode a packet with a satisfactory bit-error rate (BER) as long as the received signal-to-interference-plus-noise ratio (SINR) is higher than 5dB (i.e., $SINR_{cut-off}=5\text{dB}$), since a 5dB SINR seems a reasonable assumption based on typical coding requirements in wireless systems [29]. Although the majority of the numerical results presented in this section are focused on the example of $SINR_{cut-off} = 5\text{dB}$, we also show some example results for $SINR_{cut-off} = 7\text{dB}$ (Figure 8) and $SINR_{cut-off} = 10\text{dB}$ (Figure 9) to demonstrate the ability of our technique to work reliably with various SINR requirements.

We also evaluate the sensitivity of our proposed discriminators to the SINR deviation from the 5dB cut-off point. That is, since the thresholds designed for the discriminators are pre-set based on studying (e.g., simulating) the statistics of the IQ signal envelope assuming “cut-off” SINR of 5dB, it is important to investigate if the algorithm would still work reliably if the signal’s SINR is offset by a $\pm \Delta\text{dB}$ (e.g. $\Delta_{SINR} = \pm 1.5\text{dB}$ means the SINR =

6.5dB for calculating False-Alarm probabilities, and the $SINR = 3.5\text{dB}$ for calculating Miss probabilities when $SINR_{cut-off}$ is 5 dB). In addition, we evaluate various measurement periods (number of information bits and number of samples per symbol, i.e., over-sampling rate), as well as various levels of quantization of the PP technique computation to evaluate the performance of our technique in fixed-point implementation. We typically generate 100,000 simulation snapshots where each snapshot generates a random number of interferers up to 30 sensors with random power assignments.

Figures 6 7, 8 and 9 show the Miss (purple points) and False-Alarm (cyan points) probabilities versus the choice of the technique comparison threshold level (i.e., above which we decide the packet is valid (collision-free) and vice-versa) for the zero-power periods and the single pilot period techniques (the choice of system parameters is defined in the caption of the corresponding figure). As shown in the figures, the intersection point of the purple and cyan curves, can be a reasonable point to choose the threshold level in order to have a reasonable (or balanced) consideration of the Miss and False-Alarm probabilities, but certainly a designer can refer to Appendix A to choose an arbitrarily different point for a different criterion of choice.

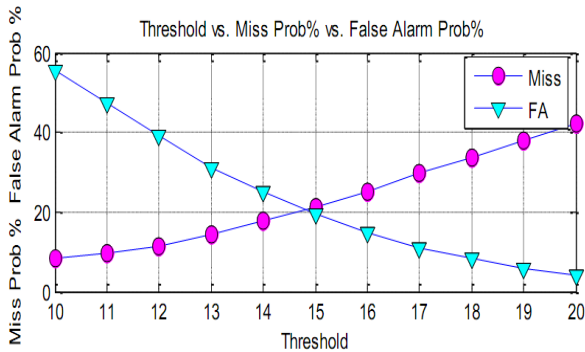


Fig.6. Miss probability =21.01% vs. False-Alarm probability=20.92% vs. threshold=15.0, $\Delta_{SINR} = \pm 1.5\text{dB}$, $SINR_{cut-off} = 5\text{dB}$, QPSK, measurement period (R)=50 bits, quantization level (B)=8, over-sampling rate(Z)=6: zero-power periods.

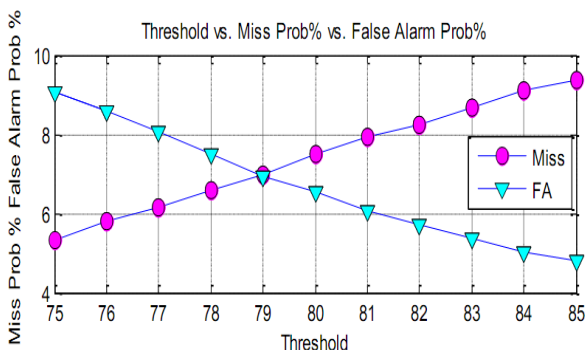


Fig.7. Miss probability =6.98% vs. False-Alarm probability=6.95% vs. threshold=79.0, $\Delta_{SINR} = \pm 1\text{dB}$, $SINR_{cut-off} = 5\text{dB}$, QPSK, measurement period= 500 bits, $v_z/v_o = 50\%$, $\kappa = 70\%$: single-pilot period.

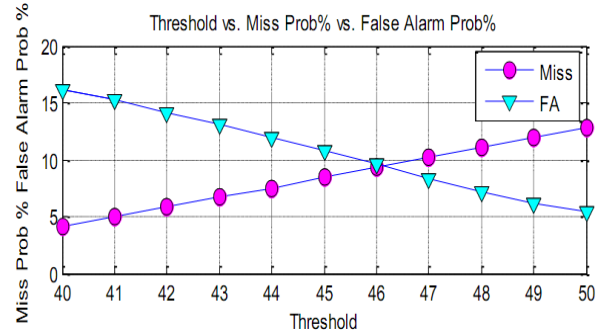


Fig.8. Miss probability = 9.88% vs. False Alarm probability=9.96% vs. threshold=46.0, $\Delta_{SINR} = \pm 1.5\text{dB}$, $SINR_{cut-off} = 7\text{dB}$, 16PSK, measurement period= 500 bits, $v_z/v_o = 50\%$, $\kappa = 60\%$: single-pilot period.

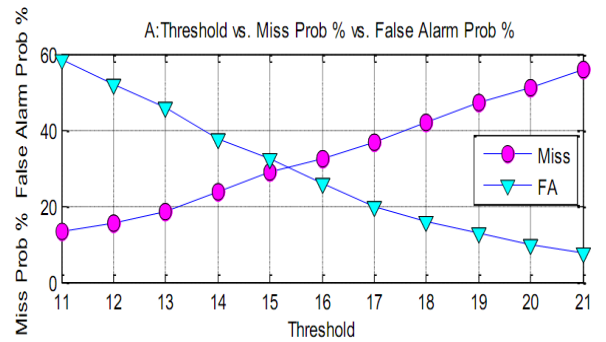


Fig.9. Miss probability =36.82% vs. False-Alarm probability=37.02% vs. threshold=15.0, $\Delta_{SINR} = \pm 1\text{dB}$, $SINR_{cut-off} = 10\text{dB}$, 8PSK, measurement period (R)=50 bits, quantization level (B)=4, over-sampling rate(Z)=2: zero-power periods.

VI. CONCLUSION

In this paper we propose novel simple power-efficient low-latency collision detection techniques for WSNs and analyze its performance. We propose two simple pilot periods techniques which are applied directly at the receiver's IQ ADC output to determine if the received signal represents a valid collision-free packet. Hence, saving a significant amount of processing power and collision detection processing time delay, compared to conventional full-decoding mechanisms, which also requires going through the entire complex receiver and modem processing. We also analyze and demonstrate the amount of power saving achieved by our PP techniques compared to the conventional full-decoding techniques. The PP techniques allow a system designer multiple degrees of freedom for design trade-offs and optimization through various design parameters.

APPENDIX

TABLES FOR SIMULATION RESULTS

In In this appendix, we provide more detailed performance results for our proposed techniques where the probability of transmissions per sensor (α)=0.3. We assume QPSK, 8PSK and 16PSK as modulation schemes. In addition, we assume $SINR_{cut-off} = 5\text{dB}$. For the single pilot period technique we assume the number of samples per slot (ω) is 2 samples. The simulation parameters are demonstrated in table I.

TABLE I
SIMULATION PARAMETERS

Simulation Parameter	Description
R	The measurement period in bits
B	The number of quantization levels for the received signal envelop
Z	The oversampling rate
G	The number of slots per pilot period
L	The length of the pilot period in single pilot period technique.
$\frac{v_z}{v_o}$	The ratio of zeros slots to ones slots in single pilot period technique.
V	The number of samples per measurement period (i.e. $Z \times \lfloor \frac{R}{M} \rfloor + L$; M is the number of information bits which are mapped to one symbol, e.g., $M=3$ for 8PSK modulation scheme)
\aleph	The soft decision percentage when decoding the received pilot sequence at the cluster head node in single pilot period technique.
Δ_{SINR}	The tolerance level for the $SINR$ (e.g. $\Delta_{SINR} = \pm 1\text{dB}$ means the $SINR = 6\text{dB}$ for calculating False-Alarm probabilities and the $SINR = 3\text{dB}$ for calculating Miss probabilities when the $SINR_{cut-off}$ is 5 dB).
P_{FA}	The probability of False-Alarm.
P_{MISS}	The probability of Miss.
γ	The threshold level as explained in section IV.

TABLE II
QPSK –ZERO-POWER PERIODS SCHEME

QPSK							
R	B	Z	Δ_{SINR}	P_{FA}	P_{MISS}	γ	V
50	4	2	$\pm 1\text{dB}$	39.72%	39.77%	11.00	56
50	8	6	$\pm 1\text{dB}$	26.16%	26.08%	15.00	156
50	10	8	$\pm 1\text{dB}$	24.57%	24.53%	16.00	206
50	4	2	$\pm 1.5\text{dB}$	36.14%	36.16%	10.00	56
50	8	6	$\pm 1.5\text{dB}$	20.92%	21.01%	15.00	156
50	10	8	$\pm 1.5\text{dB}$	19.04%	19.12%	16.00	206
100	4	2	$\pm 1\text{dB}$	26.50%	26.53%	15.00	110
100	8	6	$\pm 1\text{dB}$	20.21%	20.17%	17.00	310
100	10	8	$\pm 1\text{dB}$	18.30%	18.32%	17.00	410
100	4	2	$\pm 1.5\text{dB}$	21.08%	21.02%	15.00	110
100	8	6	$\pm 1.5\text{dB}$	14.90%	14.90%	17.00	310
100	10	8	$\pm 1.5\text{dB}$	12.20%	12.22%	17.00	410
200	4	2	$\pm 1\text{dB}$	20.00%	20.01%	17.00	220
200	8	6	$\pm 1\text{dB}$	15.83%	15.84%	18.00	620
200	10	8	$\pm 1\text{dB}$	14.08%	14.06%	19.00	820
200	4	2	$\pm 1.5\text{dB}$	15.00%	15.00%	17.00	220
200	8	6	$\pm 1.5\text{dB}$	10.18%	10.22%	18.00	620
200	10	8	$\pm 1.5\text{dB}$	9.60%	9.64%	18.00	820
500	4	2	$\pm 1\text{dB}$	14.10%	14.11%	19.00	550
500	8	6	$\pm 1\text{dB}$	11.10%	11.16%	19.00	1550
500	10	8	$\pm 1\text{dB}$	10.10%	10.15%	19.00	2050
500	4	2	$\pm 1.5\text{dB}$	12.11%	12.19%	18.00	550
500	8	6	$\pm 1.5\text{dB}$	10.15%	10.20%	18.00	1550
500	10	8	$\pm 1.5\text{dB}$	9.20%	9.22%	18.00	2050
1000	4	2	$\pm 1\text{dB}$	10.05%	10.02%	20.00	1100
1000	8	6	$\pm 1\text{dB}$	8.36%	8.30%	20.00	3100
1000	10	8	$\pm 1\text{dB}$	7.56%	7.60%	20.00	4100
1000	4	2	$\pm 1.5\text{dB}$	9.21%	9.26%	19.00	1100
1000	8	6	$\pm 1.5\text{dB}$	7.43%	7.41%	19.00	3100
1000	10	8	$\pm 1.5\text{dB}$	6.20%	6.18%	19.00	4100

TABLE III
8PSK –ZERO-POWER PERIODS SCHEME

8PSK							
R	B	Z	Δ_{SINR}	P_{FA}	P_{MISS}	γ	V
50	4	2	$\pm 1\text{dB}$	43.76%	44.45%	6.00	38
50	8	6	$\pm 1\text{dB}$	38.11%	38.19%	13.00	102
50	10	8	$\pm 1\text{dB}$	28.44%	28.40%	15.00	134
50	4	2	$\pm 1.5\text{dB}$	38.04%	38.06%	6.00	38
50	8	6	$\pm 1.5\text{dB}$	29.60%	29.61%	13.00	102
50	10	8	$\pm 1.5\text{dB}$	26.32%	26.33%	14.00	134
100	4	2	$\pm 1\text{dB}$	31.13%	31.10%	13.00	74
100	8	6	$\pm 1\text{dB}$	23.33%	23.34%	17.00	202
100	10	8	$\pm 1\text{dB}$	19.25%	19.20%	17.00	266
100	4	2	$\pm 1.5\text{dB}$	25.11%	25.10%	13.00	74
100	8	6	$\pm 1.5\text{dB}$	19.13%	19.10%	16.00	202
100	10	8	$\pm 1.5\text{dB}$	17.12%	17.13%	16.00	266
200	4	2	$\pm 1\text{dB}$	23.15%	23.12%	16.00	152
200	8	6	$\pm 1\text{dB}$	16.65%	16.60%	18.00	416
200	10	8	$\pm 1\text{dB}$	15.14%	15.17%	18.00	647
200	4	2	$\pm 1.5\text{dB}$	19.03%	19.00%	15.00	152
200	8	6	$\pm 1.5\text{dB}$	11.94%	11.92%	18.00	416
200	10	8	$\pm 1.5\text{dB}$	10.20%	10.24%	17.00	647
500	4	2	$\pm 1\text{dB}$	18.40%	18.40%	18.00	382
500	8	6	$\pm 1\text{dB}$	13.20%	13.10%	18.00	1046
500	10	8	$\pm 1\text{dB}$	17.32%	17.33%	18.00	1378
500	4	2	$\pm 1.5\text{dB}$	13.01%	13.09%	18.00	382
500	8	6	$\pm 1.5\text{dB}$	11.03%	11.00%	18.00	1046
500	10	8	$\pm 1.5\text{dB}$	10.11%	10.11%	17.00	1378
1000	4	2	$\pm 1\text{dB}$	13.12%	13.12%	18.00	766
1000	8	6	$\pm 1\text{dB}$	10.01%	10.02%	19.00	2098
1000	10	8	$\pm 1\text{dB}$	8.22%	8.21%	20.00	2764
1000	4	2	$\pm 1.5\text{dB}$	10.21%	10.24%	20.00	766
1000	8	6	$\pm 1.5\text{dB}$	8.11%	8.12%	20.00	2098
1000	10	8	$\pm 1.5\text{dB}$	7.64%	7.65%	20.00	2764

TABLE IV
16PSK –ZERO-POWER PERIODS SCHEME

16PSK							
R	B	Z	Δ_{SINR}	P_{FA}	P_{MISS}	γ	V
50	4	2	$\pm 1\text{dB}$	46.22%	46.21%	6.00	30
50	8	6	$\pm 1\text{dB}$	39.21%	39.33%	12.00	78
50	10	8	$\pm 1\text{dB}$	33.76%	33.77%	13.00	102
50	4	2	$\pm 1.5\text{dB}$	39.11%	39.13%	6.00	30
50	8	6	$\pm 1.5\text{dB}$	32.12%	32.10%	11.00	78
50	10	8	$\pm 1.5\text{dB}$	29.54%	29.51%	13.00	102
100	4	2	$\pm 1\text{dB}$	33.23%	33.30%	11.00	60
100	8	6	$\pm 1\text{dB}$	25.21%	25.22%	15.00	160
100	10	8	$\pm 1\text{dB}$	22.32%	22.32%	16.00	210
100	4	2	$\pm 1.5\text{dB}$	26.01%	26.02%	10.00	60
100	8	6	$\pm 1.5\text{dB}$	22.25%	22.21%	15.00	160
100	10	8	$\pm 1.5\text{dB}$	19.65%	19.67%	16.00	60
200	4	2	$\pm 1\text{dB}$	24.98%	24.97%	16.00	120
200	8	6	$\pm 1\text{dB}$	19.19%	19.20%	17.00	320
200	10	8	$\pm 1\text{dB}$	16.04%	16.02%	17.00	420
200	4	2	$\pm 1.5\text{dB}$	20.13%	20.09%	15.00	120
200	8	6	$\pm 1.5\text{dB}$	13.45%	12.55%	17.00	320
200	10	8	$\pm 1.5\text{dB}$	11.66%	11.64%	17.00	420
500	4	2	$\pm 1\text{dB}$	19.23%	19.21%	17.00	300
500	8	6	$\pm 1\text{dB}$	14.26%	14.22%	17.00	800
500	10	8	$\pm 1\text{dB}$	18.32%	18.36%	17.00	1050
500	4	2	$\pm 1.5\text{dB}$	14.41%	14.47%	17.00	300
500	8	6	$\pm 1.5\text{dB}$	12.63%	12.68%	17.00	800
500	10	8	$\pm 1.5\text{dB}$	11.19%	11.91%	17.00	1050
1000	4	2	$\pm 1\text{dB}$	14.66%	14.65%	18.00	600
1000	8	6	$\pm 1\text{dB}$	11.11%	11.13%	19.00	1600
1000	10	8	$\pm 1\text{dB}$	9.01%	9.00%	19.00	2100
1000	4	2	$\pm 1.5\text{dB}$	11.24%	11.24%	19.00	600
1000	8	6	$\pm 1.5\text{dB}$	9.85%	9.88%	19.00	1600
1000	10	8	$\pm 1.5\text{dB}$	8.45%	8.43%	19.00	2100

TABLE V
QPSK –SINGLE PSEUDO-CODED ON-OFF PILOT PERIOD SCHEME

QPSK												
R	B	Z	v	$\frac{vZ}{vO}$	L	V	\aleph	Δ_{SINR}	P_{FA}	P_{MISS}	γ	
50	4	2	8	0.5	16	66	60%	$\pm 1dB$	21.61%	21.62%	92.0	
								$\pm 1.5dB$	20.50%	20.83%	90.0	
	10	8	7	0.4	14	214	60%	$\pm 1dB$	22.45%	22.65%	105.0	
								$\pm 1.5dB$	21.14%	21.11%	105.0	
	4	2	8	0.5	16	66	70%	$\pm 1dB$	8.61%	8.68%	90.0	
								$\pm 1.5dB$	7.18%	7.12%	91.0	
	10	8	7	0.4	14	214	70%	$\pm 1dB$	9.25%	9.13%	105.0	
								$\pm 1.5dB$	8.20%	8.37%	105.0	
	4	2	8	0.5	16	66	90%	$\pm 1dB$	0.31%	0.33%	89.0	
								$\pm 1.5dB$	0.21%	0.20%	89.0	
	10	8	7	0.4	14	214	90%	$\pm 1dB$	0.47%	0.45%	105.0	
								$\pm 1.5dB$	0.30%	0.30%	105.0	
500	4	2	8	0.5	16	516	60%	$\pm 1dB$	19.69%	19.65%	80.0	
								$\pm 1.5dB$	18.21%	18.26%	79.0	
	10	8	7	0.4	14	2014	60%	$\pm 1dB$	20.45%	20.65%	96.0	
								$\pm 1.5dB$	19.42%	19.50%	96.0	
	4	2	8	0.5	16	516	70%	$\pm 1dB$	6.95%	6.98%	79.0	
								$\pm 1.5dB$	5.32%	5.34%	79.0	
	10	8	7	0.4	14	2014	70%	$\pm 1dB$	7.45%	7.65%	95.0	
								$\pm 1.5dB$	6.23%	6.29%	95.0	
	4	2	8	0.5	16	516	90%	$\pm 1dB$	0.29%	0.28%	77.0	
								$\pm 1.5dB$	0.18%	0.15%	77.0	
	10	8	7	0.4	14	2014	90%	$\pm 1dB$	0.44%	0.41%	88.0	
								$\pm 1.5dB$	0.28%	0.22%	88.0	
1000	4	2	8	0.5	16	1016	60%	$\pm 1dB$	18.29%	18.29%	80.0	
								$\pm 1.5dB$	17.84%	17.81%	80.0	
	10	8	7	0.4	14	4014	60%	$\pm 1dB$	19.93%	19.85%	95.0	
								$\pm 1.5dB$	18.27%	18.21%	95.0	
	4	2	8	0.5	16	1016	70%	$\pm 1dB$	5.81%	5.89%	80.0	
								$\pm 1.5dB$	4.11%	4.12%	80.0	
	10	8	7	0.4	14	4014	70%	$\pm 1dB$	6.05%	6.05%	95.0	
								$\pm 1.5dB$	5.13%	5.10%	95.0	
	4	2	8	0.5	16	1016	90%	$\pm 1dB$	0.22%	0.20%	76.0	
								$\pm 1.5dB$	0.12%	0.13%	76.0	
	10	8	7	0.4	14	4014	90%	$\pm 1dB$	0.36%	0.35%	90.0	
								$\pm 1.5dB$	0.23%	0.23%	90.0	

TABLE VII
16PSK –Single Pseudo-Coded ON-OFF Pilot Period Scheme

16PSK												
R	B	Z	G	$\frac{vZ}{vO}$	L	V	\aleph	Δ_{SINR}	P_{FA}	P_{MISS}	γ	
50	4	2	8	0.5	16	40	60%	$\pm 1dB$	19.11%	19.17%	96.0	
								$\pm 1.5dB$	18.77%	18.73%	96.0	
	10	8	7	0.4	14	110	60%	$\pm 1dB$	20.16%	20.13%	106.0	
								$\pm 1.5dB$	19.14%	19.15%	106.0	
	4	2	8	0.5	16	40	70%	$\pm 1dB$	6.69%	6.63%	92.0	
								$\pm 1.5dB$	5.86%	5.79%	92.0	
	10	8	7	0.4	14	110	70%	$\pm 1dB$	7.71%	7.73%	113.0	
								$\pm 1.5dB$	6.09%	6.03%	113.0	
	4	2	8	0.5	16	40	90%	$\pm 1dB$	0.17%	0.16%	92.0	
								$\pm 1.5dB$	0.06%	0.08%	92.0	
	10	8	7	0.4	14	110	90%	$\pm 1dB$	0.25%	0.24%	106.0	
								$\pm 1.5dB$	0.13%	0.17%	106.0	
500	4	2	8	0.5	16	266	60%	$\pm 1dB$	17.63%	17.65%	81.0	
								$\pm 1.5dB$	16.30%	16.27%	81.0	
	10	8	7	0.4	14	1014	60%	$\pm 1dB$	17.20%	17.19%	100.0	
								$\pm 1.5dB$	16.10%	16.15%	100.0	
	4	2	8	0.5	16	266	70%	$\pm 1dB$	6.94%	5.91%	81.0	
								$\pm 1.5dB$	5.02%	5.05%	82.0	
	10	8	7	0.4	14	1014	70%	$\pm 1dB$	6.14%	6.17%	102.0	
								$\pm 1.5dB$	5.13%	5.10%	102.0	
	4	2	8	0.5	16	266	90%	$\pm 1dB$	0.16%	0.18%	78.0	
								$\pm 1.5dB$	0.06%	0.04%	78.0	
	10	8	7	0.4	14	1014	90%	$\pm 1dB$	0.26%	0.29%	92.0	
								$\pm 1.5dB$	0.09%	0.11%	92.0	
1000	4	2	8	0.5	16	514	60%	$\pm 1dB$	17.08%	17.01%	82.0	
								$\pm 1.5dB$	15.64%	15.61%	82.0	
	10	8	7	0.4	14	2016	60%	$\pm 1dB$	16.07%	16.10%	98.0	
								$\pm 1.5dB$	14.68%	14.71%	98.0	
	4	2	8	0.5	16	514	70%	$\pm 1dB$	4.81%	4.84%	82.0	
								$\pm 1.5dB$	3.54%	3.52%	83.0	
	10	8	7	0.4	14	2016	70%	$\pm 1dB$	5.01%	5.05%	100.0	
								$\pm 1.5dB$	3.67%	3.70%	100.0	
	4	2	8	0.5	16	514	90%	$\pm 1dB$	0.10%	0.09%	77.0	
								$\pm 1.5dB$	0.02%	0.03%	77.0	
	10	8	7	0.4	14	2016	90%	$\pm 1dB$	0.19%	0.16%	99.0	
								$\pm 1.5dB$	0.08%	0.09%	99.0	

TABLE VI
8PSK –SINGLE PSEUDO-CODED ON-OFF PILOT PERIOD SCHEME

8PSK												
R	B	Z	G	$\frac{vZ}{vO}$	L	V	\aleph	Δ_{SINR}	P_{FA}	P_{MISS}	γ	
50	4	2	8	0.5	16	48	60%	$\pm 1dB$	20.61%	20.62%	95.0	
								$\pm 1.5dB$	19.21%	19.21%	105.0	
	10	8	7	0.4	14	142	60%	$\pm 1dB$	21.15%	21.12%	105.0	
								$\pm 1.5dB$	20.04%	20.05%	105.0	
	4	2	8	0.5	16	48	70%	$\pm 1dB$	7.29%	7.23%	89.0	
								$\pm 1.5dB$	6.85%	6.75%	89.0	
	10	8	7	0.4	14	142	70%	$\pm 1dB$	9.41%	8.43%	110.0	
								$\pm 1.5dB$	7.20%	7.17%	110.0	
	4	2	8	0.5	16	48	90%	$\pm 1dB$	0.23%	0.22%	91.0	
								$\pm 1.5dB$	0.14%	0.17%	91.0	
	10	8	7	0.4	14	142	90%	$\pm 1dB$	0.37%	0.32%	104.0	
								$\pm 1.5dB$	0.21%	0.23%	104.0	
500	4	2	8	0.5	16	348	60%	$\pm 1dB$	18.19%	18.15%	80.0	
								$\pm 1.5dB$	17.13%	17.20%	79.0	
	10	8	7	0.4	14	1342	60%	$\pm 1dB$	18.97%	18.95%	99.0	
								$\pm 1.5dB$	17.12%	17.10%	98.0	
	4	2	8	0.5	16	348	70%	$\pm 1dB$	6.05%	6.01%	80.0	
								$\pm 1.5dB$	5.12%	5.14%	80.0	
	10	8	7	0.4	14	1342	70%	$\pm 1dB$	6.95%	6.97%	99.0	
								$\pm 1.5dB$	5.43%	5.50%	99.0	
	4	2	8	0.5	16	348	90%	$\pm 1dB$	0.19%	0.20%	77.0	
								$\pm 1.5dB$	0.14%	0.13%	77.0	
	10	8	7	0.4	14	1342	90%	$\pm 1dB$	0.34%	0.35%	90.0	
								$\pm 1.5dB$	0.18%	0.19%	90.0	
1000	4	2	8	0.5	16	682	60%	$\pm 1dB$	17.98%	17.91%	80.0	
								$\pm 1.5dB$	16.34%	16.31%	80.0	
	10	8	7	0.4	14	2678	60%	$\pm 1dB$	17.13%	17.15%	99.0	
								$\pm 1.5dB$	16.56%	16.51%	98.0	
	4	2	8	0.5	16	682	70%	$\pm 1dB$	5.01%	5.09%	80.0	
								$\pm 1.5dB$	4.01%	4.02%	80.0	
	10	8	7	0.4	14	2678	70%	$\pm 1dB$	5.95%	5.85%	99.0	
								$\pm 1.5dB$	4.53%	4.50%	99.0	
	4	2	8	0.5	16	682	90%	$\pm 1dB$	0.20%	0.19%	76.0	
								$\pm 1.5dB$	0.08%	0.09%	76.0	
	10	8	7	0.4	14	2678	90%	$\pm 1dB$	0.26%	0.28%	98.0	
								$\pm 1.5dB$	0.14%	0.13%	98.0	

REFERENCES

- [1] Kori, R.H.; Angadi, A.S.; Hiremath, M.K.; Iddalagi, S. M., "Efficient Power Utilization of Wireless Sensor Networks: A Survey," Advances in Recent Technologies in Communication and Computing, 2009. ARTCom '09. International Conference on , vol., no., pp.571,575, 27-28 Oct. 2009.
- [2] Zorzi, M.; Rao, R.R., "Coding tradeoffs for reduced energy consumption in sensor networks," Personal, Indoor and Mobile Radio Communications, 2004. PIMRC 2004. 15th IEEE International Symposium on, vol.1, no., pp.206,210 Vol.1, 5-8 Sept. 2004.
- [3] Harry L. Van Trees. Detection, Estimation, and Modulation Theory: Part I, John Wiley and Sons, 1968 .
- [4] Chen, J.; Abedi, A., "Distributed Turbo Coding and Decoding for Wireless Sensor Networks," Communications Letters, IEEE , vol.15, no.2, pp.166,168, February 2011.
- [5] Chanchal Kr. Dey and Sumit Kundu , "Hybrid Forwarding for General Cooperative Wireless Relaying in m-Nakagami Fading Channel", International Journal of Future Generation Communication and Networking Vol.5,No.1,March,2012.
- [6] Guogang Hua; Chang Wen Chen, "Distributed source coding in wireless sensor networks," Quality of Service in Heterogeneous Wired/Wireless Networks, 2005. Second International Conference on, vol., no., pp.7 pp.,6, 24-24 Aug. 2005.
- [7] Robertson, P.; Villebrun, E.; Hoehner, P., "A comparison of optimal and sub-optimal MAP decoding algorithms operating in the log domain," Communications, 1995. ICC '95 Seattle, 'Gateway to Globalization', 1995 IEEE International Conference on , vol.2, no., pp.1009,1013 vol.2, 18-22 Jun,1995.
- [8] Cam, H., "Multiple-Input Turbo Code for Joint Data Aggregation, Source and Channel Coding in Wireless Sensor Networks," Communications, 2006. ICC'06. IEEE International Conference on, vol.8, no., pp.3530,3535, June 2006.
- [9] T.V. Dam and K. Langendoen, "An Adaptive Energy-Efficient MAC Protocol for Wireless Sensor Networks", The First ACM Conference on Embedded Networked Sensor Systems (Sensys'03), Los Angeles, CA, USA, November 2003.
- [10] Jun Peng; Liang Cheng; Sikdar, B., "A Wireless MAC Protocol with Collision Detection," Mobile Computing, IEEE Transactions on , vol.6, no.12, pp.1357,1369, Dec. 2007.

- [11] F. A. Tobagi and L. Kleinrock, "Packet switching in radio channels: Part II - the hidden terminal problem in carrier sense multiple access and the busy tone solution," *IEEE Transactions on Communications*, vol. 23, pp. 1417-1433, 1975.
- [12] I. F. Akyildiz et al., "Wireless sensor networks: a survey", *Computer Networks*, Vol. 38, pp. 393-422, March 2002.
- [13] W. Ye, J. Heidemann, D. Estrin, "Medium Access Control With Coordinated Adaptive Sleeping for Wireless Sensor Networks", *IEEE/ACM Transactions on Networking*, Volume: 12, Issue: 3, Pages: 493 - 506, June 2004.
- [14] K. Jamieson, H. Balakrishnan, and Y. C. Tay, "Sift: A MAC Protocol for Event-Driven Wireless Sensor Networks", MIT Laboratory for Computer Science, Tech. Rep.894, May 2003.
- [15] G. Lu, B. Krishnamachari, C.S. Raghavendra, "An adaptive energy efficient and low-latency MAC for data gathering in wireless sensor networks", *Proceedings of 18th International Parallel and Distributed Processing Symposium*, Pages: 224, 26-30 April 2004.
- [16] P. Lin, C. Qiao, and X. Wang, "Medium access control with a dynamic duty cycle for sensor networks", *IEEE Wireless Communications and Networking Conference*, Volume: 3, Pages: 1534 - 1539, 21-25 March 2004.
- [17] Sandra, S.; Jaime, L.; Miguel, G.; Jose, F.T, "Power Saving and Energy Optimization Techniques for Wireless Sensor Networks (Invited Paper)." *Journal of Communications*, vol. 6. No.6, pp.439-459, 2011.
- [18] Sungoh Kwon; Shroff, N.B., "Energy-Efficient Interference-Based Routing for Multi-Hop Wireless Networks," *INFOCOM 2006. 25th IEEE International Conference on Computer Communications. Proceedings*, vol., no., pp.1,12, April 2006.
- [19] da S Araújo, H.; HolandaFilho, R.; Filho, R.H., "WSN Routing: An Geocast Approach for Reducing Consumption Energy," *Wireless Communications and Networking Conference (WCNC), 2010 IEEE*, vol., no., pp.1,6, 18-21 April 2010.
- [20] El-Aaasser, M.; Ashour, M., "Energy aware classification for wireless sensor networks routing," *Advanced Communication Technology (ICACT), 2013 15th International Conference on*, vol., no., pp.66,71, 27-30 Jan. 2013.
- [21] Cardei, M.; Thai, M.T.; Yingshu Li; Weili Wu, "Energy-efficient target coverage in wireless sensor networks," *INFOCOM 2005. 24th Annual Joint Conference of the IEEE Computer and Communications Societies. Proceedings IEEE*, vol.3, no., pp.1976,1984 vol. 3, 13-17 March 2005.
- [22] Junchao Ma; Wei Lou; Yanwei Wu; Mo Li; Guihai Chen, "Energy Efficient TDMA Sleep Scheduling in Wireless Sensor Networks," *INFOCOM 2009, IEEE*, vol., no., pp.630,638, 19-25 April 2009.
- [23] Ingelrest, F.; Simplot-Ryl, D.; Stojmenovic, I., "Smaller Connected Dominating Sets in Ad Hoc and Sensor Networks based on Coverage by Two-Hop Neighbors," *Communication Systems Software and Middleware, 2007. COMSWARE 2007. 2nd International Conference on*, vol., no., pp.1,8, 7-12 Jan. 2007.
- [24] Heinzelman, W.R.; Chandrakasan, A.; Balakrishnan, H., "Energy-efficient communication protocol for wireless microsensor networks," *System Sciences, 2000. Proceedings of the 33rd Annual Hawaii International Conference on*, vol., no., pp.10 pp. vol.2,, 4-7 Jan. 2000.
- [25] Li, N.; Hou, J.C.; LuiSha, "Design and analysis of an MST-based topology control algorithm," *Wireless Communications, IEEE Transactions on*, vol.4, no.3, pp.1195,1206, May 2005.
- [26] Chen, J.; Abedi, A., "Distributed Turbo Coding and Decoding for Wireless Sensor Networks," *Communications Letters, IEEE*, vol.15, no.2, pp.166,168, February 2011.
- [27] Liang Li; Maunder, R.G.; Al-Hashimi, B.M.; Hanzo, L., "A Low-Complexity Turbo Decoder Architecture for Energy-Efficient Wireless Sensor Networks," *Very Large Scale Integration (VLSI) Systems, IEEE Transactions on*, vol.21, no.1, pp.14,22, Jan. 2013.
- [28] Robertson, P.; Villebrun, E.; Hoeher, P., "A comparison of optimal and sub-optimal MAP decoding algorithms operating in the log domain," *Communications, 1995. ICC '95 Seattle, 'Gateway to Globalization', 1995 IEEE International Conference on*, vol.2, no., pp.1009,1013 vol.2, 18-22 Jun,1995.
- [29] Chanchal Kr. Dey and Sumit Kundu, "Hybrid Forwarding for General Cooperative Wireless Relaying in m-Nakagami Fading Channel", *International Journal of Future Generation Communication and Networking* Vol.5,No.1, March, 2012.
- [30] Fawaz Alassery, Walid K. M. Ahmed, Mohsen Sarraf and Victor Lawrence, "Novel Low-Complexity and Power-Efficient Techniques for Fast Collision Detection in Wireless Sensor Networks", *Lecture Notes in Engineering and Computer Science: Proceedings of The World Congress on Engineering 2015*, 1-3 July, 2015, London, U.K., pp 627-633.